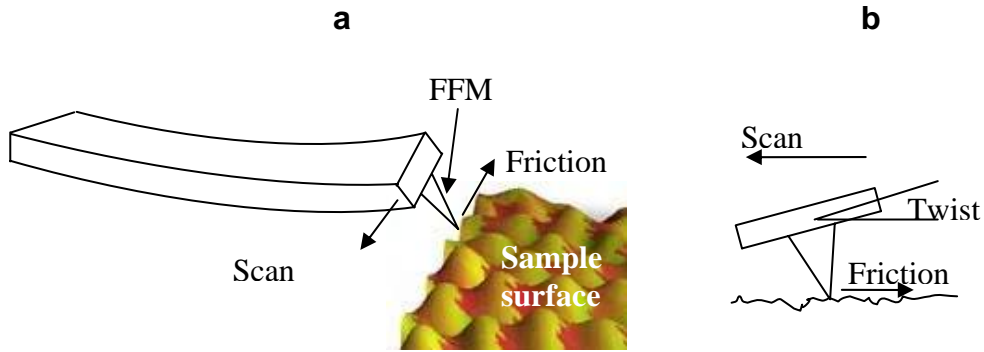


### A.1. Coupled Flexural-Torsional Nonlinear Vibrations of PZT-actuated Microcantilevers:

Planar dynamics of microcantilever beams have been investigated by many researchers. In addition, the problem of vibrations of microcantilevers has received a considerable attention since it appears in several scientific and industrial applications, such as Atomic Force Microscopy (AFM), Nanomechanical cantilever sensors (NMCS) and Friction Force Microscopy (FFM). Utilizing microcantilevers provides the ability to rapidly detect small quantities of materials in different environment such as gas or liquid. The microcantilever beam vibration spectrum has been used to detect a target mass particle attached eccentrically to the beam which produces both flexural and torsional vibrations.

In both FFM and AFM, a microcantilever beam with a sharp tip is utilized (as shown in Fig. 8-a) for acquiring topographic information from the surface through mechanical interaction between microcantilever tip and sample. While mostly flexural vibrations occur in AFM, FFM may experience torsional vibration in addition to bending. This is due to the fact that the scanning direction in FFM is perpendicular to beam length and the tip of the beam. The resulting friction force twists the tip of the beam producing torsion in the beam as shown in Fig. 8-b. It is shown here that the torsion is coupled with flexure because of the nonlinear geometry and presence of piezoelectric actuator. In addition, an indirect method for measuring the friction force is presented.



**Fig. 8** (a) Schematic operation of FFM, and (b) twist of the FFM tip, [8].

As shown in Fig. 9, the piezoelectric layer is not bounded on the entire length of the beam; therefore, the neutral surface varies for each section. For  $s < l_1$  or  $s > l_2$  where piezoelectric is not attached, the neutral surface is the geometric center of the beam ( $y_n = 0$ ). The position of neutral surface,  $y_n$ , for the section where piezoelectric layer is attached can be obtained as

$$y_n = \frac{E_p h_p (h_p + h_b)}{2(E_p h_p + E_b h_b)}$$

where  $h$  indicates the beam thickness and the subscripts  $b$  and  $p$  denote the beam material and piezoelectric layer properties, respectively and  $w$  is the beam width.

The coupling relation between the stress and the electrical field for piezoelectric layer is expressed as

$$\sigma_{11}^p = E_p \varepsilon_{11}^p - E_p d_{31} \frac{P(t)}{h_p},$$

where  $P(t)$  is applied voltage to the piezoelectric material.

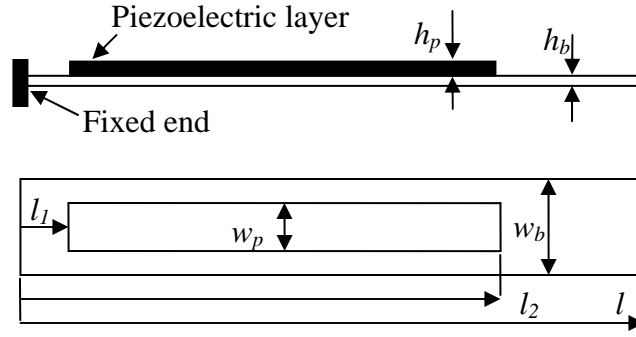


**Fig. 9** Geometry of the microcantilever beam [8].

An energy method is utilized here to derive the equations of motion. Utilizing the Lagrangian method, the equations of motion of the system with respect to three variables  $u$  (longitudinal vibration),  $\phi$  (torsional vibration), and  $v$  (bending vibration) can be obtained as [8, 9]

$$(J_\theta - J_\zeta)\phi\ddot{v}'^2 - (C_\theta - C_\zeta)\phi v''^2 + (C_\xi\phi')' - \frac{1}{2}C_c v''\phi P(t) = J_\xi\ddot{\phi},$$

$$\phi = 0 \text{ at } s = 0 \quad ; \quad \phi' = 0 \text{ at } s = l,$$

$$\left[ \frac{1}{2}C_c v''P(t) + J_\zeta\dot{v}'^2 + EA\left(u' + \frac{1}{2}v'^2\right) - C_\zeta v''^2 \right]' + \left( C_\zeta v'v'' - \frac{1}{2}C_c v'P(t) \right)'' = m\ddot{u},$$

$$u = 0 \text{ at } s = 0 \quad ; \quad u' = 0 \text{ at } s = l,$$

$$\left[ J_\zeta(\dot{u}'\dot{v}' + 2v'\dot{v}'^2) - C_\zeta(u''v'' + 2v'v''^2) + EA\left(u'v' + \frac{1}{2}v'^3\right) + C_c\left(\frac{1}{2}u'' + v''v'\right)P(t) \right]' - \left[ C_\theta v''\phi^2 + C_\zeta(v'' - v''\phi^2 - 2v''v'^2 - 2v''u' - v'u'') - \frac{1}{2}C_c\left(1 - u' - v'^2 - \frac{\phi^2}{2}\right)P(t) \right]'' + \frac{\partial}{\partial t} \left[ J_\theta\dot{v}'\phi^2 + J_\zeta(\dot{v}' - \dot{v}'\phi^2 - 2u'\dot{v}' - \dot{u}'v' - 2\dot{v}'v'^2) \right]' = m\dot{v}$$

$$v = v' = 0 \text{ at } s = 0 \quad ; \quad v'' = v''' = 0 \text{ at } s = l.$$

As seen from these equations, there exist nonlinear terms in the equations from order two to three. However, the nonlinearities of the second order are due to presence of piezoelectric layer. Considering the equations of motion, it is observed the torsional and flexural vibrations are coupled in two ways; one is a third order nonlinearity coupling due to beam geometry and the other one is a second order nonlinearity due to both geometry and electromechanical coupling of piezoelectric layer. The former nonlinear terms have been obtained in previous studies, while the latter is a new observation which is disclosed for the first time here. Having the equations of motion, a number of case studies are considered next to study the coupling of flexural and torsional vibration in presence of piezoelectric actuator patch and effect of nonlinearity due to beam geometry. The inextensibility condition expresses that the elongation of the neutral axis during the vibration is ignorable. Considering the inextensibility condition, the governing equations on longitudinal and flexural vibrations can be reduced into one equation consequently. Then, the equations of motion of the system can be presented in the following form [8]

$$(J_\theta - J_\zeta)\phi\dot{v}'^2 - (C_\theta - C_\zeta)\phi v''^2 + (C_\zeta\phi')' - \frac{1}{2}C_c v''\phi P(t) = J_\zeta\ddot{\phi},$$

$$\phi = 0 \quad \text{at } s=0; \quad \phi' = 0 \quad \text{at } s=l,$$

$$\begin{aligned} & \left[ \frac{1}{2}v'[C_c v'P(t)]' - v'(C_\zeta v'v'')' - mv' \int_0^s \int_0^s (\ddot{v}'v' + \dot{v}'^2) ds ds \right]' \\ & - \left[ C_\theta v''\phi^2 + C_\zeta(v'' - v''\phi^2) - \frac{1}{2}C_c \left(1 - \frac{v'^2}{2} - \frac{\phi^2}{2}\right) P(t) \right]'' \\ & + \frac{\partial}{\partial t} [J_\theta \dot{v}'\phi^2 + J_\zeta (\dot{v}' - \dot{v}'\phi^2)] = m\ddot{v} \end{aligned}$$

$$v = v' = 0 \quad \text{at } s=0; \quad v'' = v''' = 0 \quad \text{at } s=l.$$

Using the coupling of stretching and flexure to the inextensibility condition, the two nonlinear equations for longitudinal and flexure vibrations are combined into one. There are now two orders of nonlinearities, the second order nonlinearity is due to presence of piezoelectric layer and the third order nonlinear terms are due to geometry and appears as nonlinear inertia and stiffness terms.

In order to produce the ordinary differential equations governing the time functions of equations of motion, these equations are separated into position and time components using Galerkin approximation as

$$\begin{aligned} \phi(s, t) &= \sum_{m=1}^{\infty} \phi_m(s, t) = \sum_{m=1}^{\infty} \alpha_m(s) q_m(t), \\ v(s, t) &= \sum_{n=1}^{\infty} v_n(s, t) = \sum_{n=1}^{\infty} \beta_n(s) r_n(t), \end{aligned}$$

where  $\alpha_m$  and  $\beta_n$  are the comparison functions (satisfying only beam boundary conditions and not necessarily the equations of motion) for bending and torsion of the microcantilever beam and  $q_n$  are the generalized time-dependent coordinates. The ordinary differential equations governing the torsion and flexure vibration are respectively:

$$k_{1mn}\ddot{q}_m + k_{2mn}q_m + k_{3mn}q_m r_n^2 + k_{4mn}q_m r_n P(t) = 0,$$

$$k_{5mn}\ddot{r}_n + k_{6mn}r_n + k_{7mn}r_n^2 P(t) + k_{8mn}r_n^3 + k_{9mn}(r_n^2\ddot{r}_n + r_n\dot{r}_n^2) + k_{10mn}r_n q_m^2 + k_{11mn}q_m^2 P(t) = k_{12mn}P(t).$$

where  $k_{imn}$  are constants that can be obtained by orthogonality condition.

An experimental setup is designed for the nonlinear coupled flexural-torsional vibrations of the microcantilever beam. The experiment aims at finding the coupled flexural-torsional vibration frequency. For this purpose, a DMASP<sup>®</sup> microcantilever beam made by Veeco<sup>®</sup> Instruments is utilized as depicted in Fig. 10.

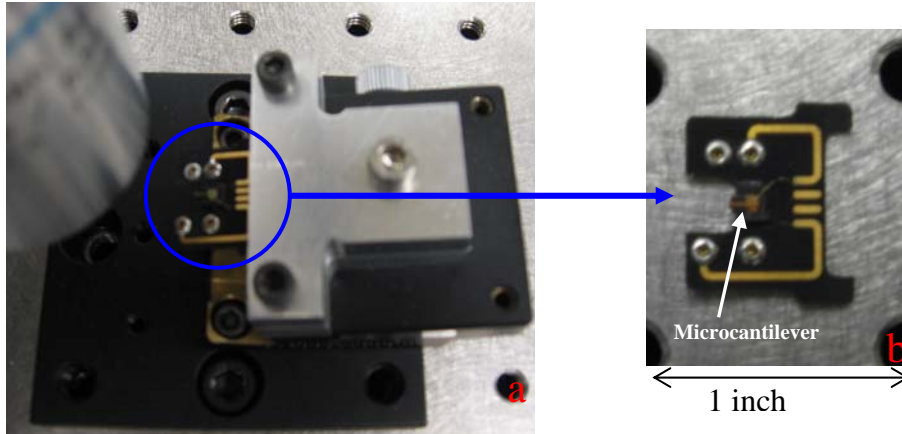


**Fig. 10** (a) The setup for experiment, and (b) microcantilever beam [8].

In order to perform the experiment, our state-of-the-art MRI, the Micro System Analyzer (MSA-400) as depicted in Fig. 11-a is used for non-contact measurement of three-dimensional motions in the microcantilever. The laser interferometry measures the out-of-plane vibration of the microcantilever tip. Using MSA-400, one can precisely adjust the laser light on the beam tip, as shown in Fig 11-b.

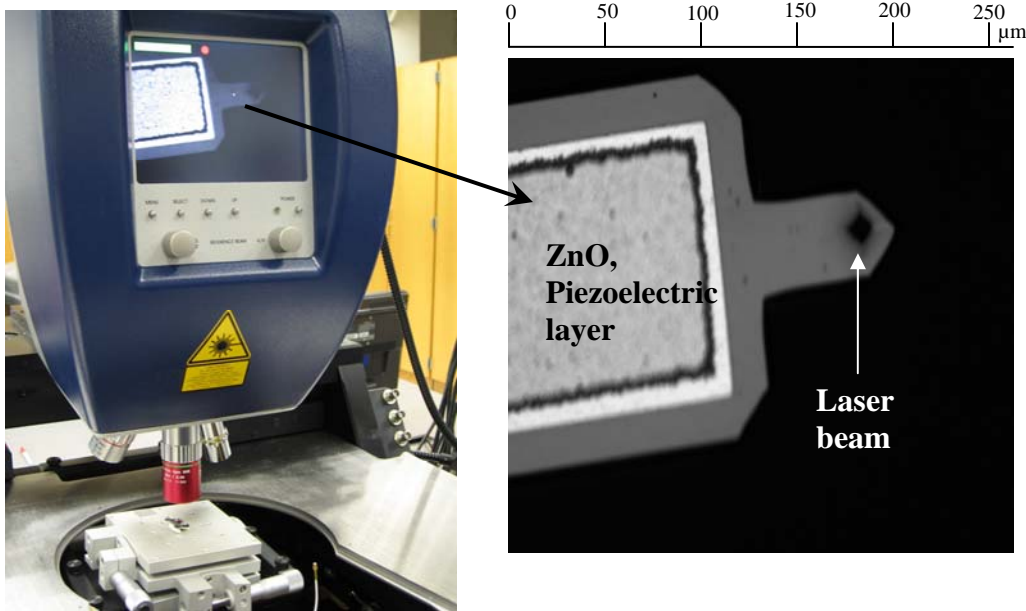


**Fig. 11** (a) The Polytec MSA-400 testing device, and (b) the tip of the microcantilever beam [8].

The DMASP<sup>®</sup> microcantilever utilized in the experimental tests has a smaller width at the end when compared with the rest of the microcantilever (see Fig. 11-b). There is a small tip vertical to the elongation of the microcantilever at its end, which is used in AFM applications. The piezoelectric layer consists of a 3.5 $\mu\text{m}$  ZnO layer and two Ti/Au layers of 0.25 $\mu\text{m}$  height on top and beneath the ZnO layer at the base of each probe.

The microcantilever is installed under the MSA-400 on the setup shown in Fig. 10 in order to use the laser light for measuring the beam vibration. The microcantilever beam vibration is then measured in response to a 1 Volt AC voltage applied to the piezoelectric layer as the excitation source. As a demonstrable example, the experimental results for first flexural natural frequency are depicted in Fig. 12.

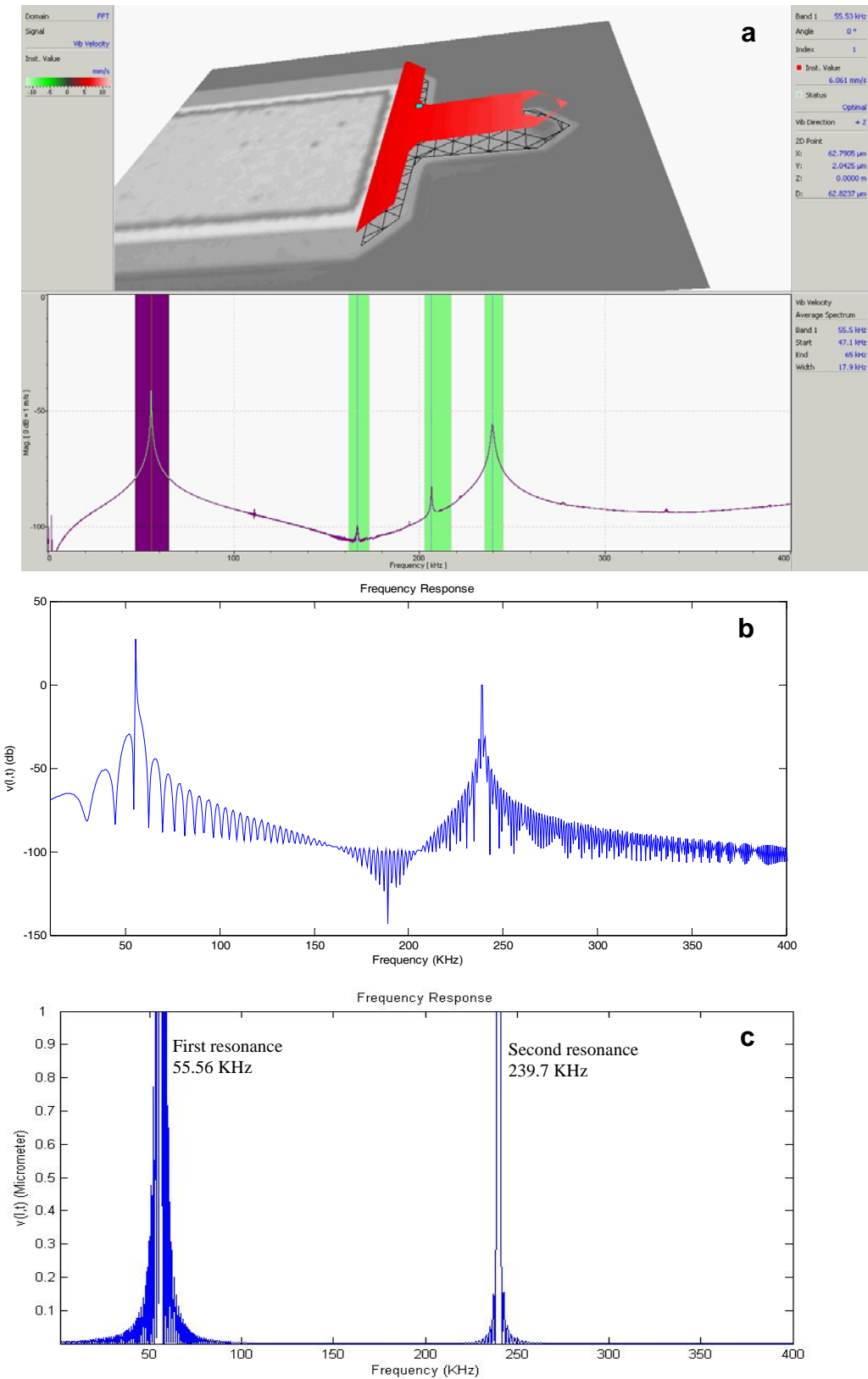


**Fig. 12** a) Experimental result, b) and c) logarithmic and linear simulation results respectively for 1 Volt chirp excitation signal with first flexural natural frequency highlighted [8].

This subtask has resulted in the following publications during this report period.

- [8] **Mahmoodi, S.N.**, and Jalili, N., “Coupled Flexural-Torsional Nonlinear Vibrations of Piezoelectrically-Actuated Microcantilevers”, accepted pending revision, *ASME Journal of Vibration and Acoustics* (May 2007).
- [9] **Mahmoodi, S.N.** and Jalili, N., “Coupled Flexural-Torsional Nonlinear Vibrations of Microcantilever Beams”, *Proceedings of the 14<sup>th</sup> International SPIE 2007 Smart Structures & Materials Conference*, San Diego, CA (February 2007).